Soil & Tillage Research 198 (2020) 104543

Contents lists available at ScienceDirect

Soil & Tillage Research

journal homepage: www.elsevier.com/locate/still

Nitrogen transformation processes and gaseous emissions from a humic gley soil at two water filled pore spaces

E. Clagnan[a,b,c,*], S.A. Rolfe[d], S.F. Thornton[b], D. Krol[a], K.G. Richards[a], G. Lanigan[a], P. Tuohy[e], O. Fenton[a]

[a] Teagasc, Environmental Research Centre, Johnstown Castle, Co. Wexford, Ireland
[b] University of Sheffield, Groundwater Protection and Restoration Group, Kroto Research Institute, Sheffield, UK
[c] Free University of Bozen-Bolzano, Faculty of Science and Technology, Bolzano, Italy
[d] University of Sheffield, Department of Animal and Plant Science, Sheffield, UK
[e] Teagasc, Animal and Grassland Research and Innovation Centre, Moorepark, Co. Cork, Ireland

ARTICLE INFO

Keywords:
Enriched fertiliser
Nitrous oxide
Isotopes
Greenhouse gases
qPCR

ABSTRACT

The artificial drainage of heavy textured gley soils is prevalent on pasture. Drainage of a soil profile reduces the water filled pore space (WFPS) in the upper soil horizons with consequences for N_2 and N_2O emissions, the fate of nitrogen (N), transformational processes and microbial and bacterial communities. The present intact soil column study with isotopically enriched fertiliser investigates all these aspects simultaneously under two WFPS treatments (80% (HS) and 55% (LS) saturation). Results showed significant differences in nitrous oxyde (N_2O) emissions, in both pattern and amount, with maxima at 11.97 mg N_2O-N/m^2h for HS and at 1.64 for LS. Isotopic enrichment data showed a significant predominance (74.8–97.2%) of nitrification in LS, with a possible reduction in NH_4^+ but a higher concentration of nitrate (NO_3^-) in N losses. Denitrification dominated in HS (72.5–73.4%), possibly leading to high ammonium (NH_4^+) losses. Enrichment values showed differential apportionment patterns. A high component of N_2O emission derived from denitrification in HS (6.0% HS; 0.4% LS) with a significant amount of N_2O (62.9%) transformed to N_2 (3.7% LS). A higher percentage of ^{15}N was retained in LS soil. HS showed a lower amount of unaccounted N highlighting lower losses. Differences in gene copy concentrations (GCC) were found across most analysed genes (*16S, nirS, nirK, nosZ1, nosZ2, amoA* and *nrfA*). Both HS and LS treatments showed similar potentials for N_2O production and its reduction to N_2, but a reduced potential for nitrification and dissimilatory nitrate reduction to ammonium (DNRA) in HS. This study explained the effect of drainage and rewetting on gaseous emissions providing an explanation in terms of community switches. On the current soil type, structures to manage watertable heights would push the system towards complete denitrification with only N_2 production but may present risks in terms of ammonia (NH_3) and NH_4^+ losses.

1. Introduction

In high rainfall pasture regions such as North Atlantic Europe, grass utilisation on heavy textured soils can be improved using artificial drainage. Surface water or groundwater gleys dominate heavy textured soils. Surface water gleys are characterised by an impermeable layer more than 40 cm below the mineral layer which does not allow vertical water permeation. Groundwater gleys have an impermeable layer located above lower permeable layers that enable the rise of groundwater. Installation of a drainage system in these soils aims to decrease the level of wetness within the profile (Tuohy et al., 2018). In the upper soil horizons, the WFPS mimics different watertable positions and therefore different positions exist in drained versus un-drained soil profiles. This alters the bioremediation functional capacity of the drained layers. This alteration of physiochemical parameters modifies microbial activities and transformational processes and alters the amount of gases emitted from the soil surface (e.g. di-nitrogen (N_2) or N_2O (Ruehle et al., 2015). In order to guide management, avoid pollution swapping and reduce N losses to the environment, the impact of natural flooding and drainage on N_2O emissions in heavy textured soils needs greater study.

Nitrification and denitrification are the main processes that attenuate NH_4^+ and NO_3^- contamination. Denitrification is a multiple step process that can release various environmentally harmful

* Corresponding author at: Free University of Bozen-Bolzano, Faculty of Science and Technology, Bolzano, Italy.
E-mail address: elisa.clagnan@unibz.it (E. Clagnan).

https://doi.org/10.1016/j.still.2019.104543
Received 14 July 2019; Received in revised form 8 November 2019; Accepted 13 December 2019
Available online 20 December 2019

intermediate products depending on environmental conditions e.g. elevated NO_3^- or dissolved oxygen (DO) concentrations might lead to the release of greenhouse gases (i.e. N_2O and nitric oxide (NO)) (Knowles, 1982). Even though denitrifiers are ubiquitous in both soil and fresh water, denitrification requires specific environmental conditions controlled by edaphic factors to occur (Hallin et al., 2009). Other processes of the N cycle occur under similar conditions as denitrification (e.g. DNRA) while others affect denitrification in terms of availability of substrates (e.g. nitrification, anammox).

The measurement of N_2 emissions indicates the quantities of N that are released to the environment during the final step of denitrification. However, since N_2 is not a greenhouse gas and its atmospheric background is 79%, it is difficult to measure and pick up small subtle changes over time (Groffman et al., 2006; Yang and Silver, 2011). In fact only a few studies document N_2 emissions (e.g. Bergstermann et al., 2011; Cardenas et al., 2017). In order to evaluate N_2 fluxes it is necessary to utilise enclosure techniques where the sample is incubated and/or the substrate is labelled (Groffman et al. 2016). On the other hand, N_2O emissions have been analysed across different WFPS scenarios (Bateman and Baggs, 2005; Rafique et al., 2011; Decock and Six, 2013). Across multiple grassland sites in Ireland, high N_2O emissions were registered in concomitance with high WFPS and soil temperature and fertiliser application (Rafique et al., 2011). According to these studies, N_2O emission and the rate of its conversion to N_2 varied according to soil type with higher emissions and lower rates evident at low WFPS. However, each soil type exhibits different characteristics, which then modify the threshold for N_2O and N_2 emission. This phenomenon requires further investigation to guide future site management (van Groenigen et al., 2004; Lesschen et al., 2011). The analyses of gas emissions coupled with ^{15}N labelled fertiliser have been able to detect the contribution of nitrification and denitrification processes to N_2O emissions. Bateman and Baggs (2005), using labelled fertiliser in a silt loam incubation, showed that WFPS below 20% limited substrate movement thereby limiting bacterial processes and N_2O emissions to anaerobic microsites. In a WFPS range from 20 to 35%, N_2O production increased significantly with nitrification becoming the dominant process at 35%. N_2O production peaked between 60–80%, with gradually increasing rates of denitrification however nitrification remained the dominant process. Cardenas et al. (2017) showed that these thresholds vary across soil textural classes and therefore comparison of results must factor in soil type. Baily et al. (2012) measured N_2O and N_2 fluxes on a moderately to well drained fine loam over clay loam textured soil with a gas chamber experiment using labelled fertiliser ($^{14}NH_4{}^{15}NO_3$: 100 kg N/ha). Results showed that mean values for N_2O and N_2 emissions for the first five days after fertilisation were dominated by N_2O produced through denitrification. However, outside of direct fertilisation application, nitrification was dominant under milder and wetter conditions.

The WFPS is also a key parameter driving microbial community structure (Fierer et al., 2003) as such communities are sensitive to environmental disturbance with changes to the community structure followed by a variation in process rates (Allison and Martiny, 2008; Giles et al., 2012). However, their analysis is essential when coupled with gaseous emissions to pinpoint the drivers and timing of such variations in transformational processes, which ultimately lead to differential N emissions. In wetland (silty clay loam; mineral) and terrestrial (silt loam; peat) ecosystems, major differences have been encountered in both microbial communities and N_2O emissions, with saturated soils enhancing denitrification when compared with unsaturated soils (Well et al., 2001; Peralta et al., 2013). Numerous soil studies have analysed the spatial pattern of the denitrifier community. For example, Philippot et al. (2009) showed spatial patterns of denitrifiers abundances based upon soil properties and land management criterion, with *nosZ* clade 1 (Jones et al., 2013) (gene involved in bacterial denitrification) emerging as a strong predictor of denitrification (the more *nosZ1* present the fuller denitrification occurs, i.e. N_2 production, and greater sustainability). However, further studies need to be carried out to assess the impact of *nosZ* on N_2O emissions. In Sweden utilising soil from an organic farm, Enwall et al. (2010) found spatial autocorrelation for the denitrifier community structure, size and activity; genes involved in bacterial denitrification (*nirK* and *nirS*) correlated with the potential rate of nitrite (NO_2^-) conversion to N_2O and the *nirS/nirK* ratio identified a particular environmental niche. Using wetland sediments in Ohio, USA, Song et al. (2010) showed that bacterial structure changed due to long term wet/dry cycles rather than short lived episodic periods and *nirS* abundance was affected by such wet-dry cycles. However, the structure was not found to be a determinant of denitrification rates due to the redundancy of this process. Regan et al. (2011), utilising grassland soils in Germany, found that the ratio of *nosZ/nirK* could be used as an indicator of N_2O emissions and therefore could be used to interpret the level of completeness of denitrification. The *amoA* gene and the potential nitrification rates have been previously positively correlated in soil with increase in the production intensities and N-inputs (Stempfhuber et al., 2014). Anammox bacteria are common in water-saturated agricultural soils with high N availability (Humbert et al., 2010), however they are generally not considered a main N_2 production process within agricultural soils (Long et al., 2013). Limited research with respect to the DNRA process (exception Morrissey et al., 2013) is available within the literature and where present conclusions are inconclusive or contradict each other (e.g. Welsh et al., 2014; Bu et al., 2017).

It still remains unclear how a) the effect of drainage on heavy textured soils and b) the driving community affect N_2 and N_2O fluxes. These knowledge gaps make it difficult to implement mitigation guidelines for farmers as artificially draining soils with lower hydraulic conductivities enables greater infiltration of water and dissolved oxygen (DO) into the soil profile, which may induce contamination and/or pollution swapping in shallow groundwater. Herein, intact soil columns (to reflect in situ soil properties and structure) were collected from an intensive farm characterised by gleic soils with the flooding-draining process simulated in a microcosm experiment. The purpose of this experiment was to understand the microbial drivers of N_2O emission and their activities under varied water conditions. A combination of flux analysis, ^{15}N stable isotope techniques and molecular techniques has been used to improve our understanding and validate the contribution of each process involved in N_2O production/consumption (Decock and Six, 2013). The objectives of the present intact column study across two WFPS treatments were to 1) assess differences in N_2 and N_2O emissions and in transformational processes on heavy textured soil, 2) trace the fate of N and 3) investigate the microbial community and the impact of the treatments on bacterial community by the analyses of *16S RNA, nirS, nirK, nosZ1, nosZ2, amoA, hzo1* and *nrfA* gene abundances.

2. Materials and methods

2.1. Site selection

The site (2.1 ha, Co. Limerick, 52°45′, 09°30′) is indicative of a poorly drained humic surface water gley, with high annual rainfall (e.g. 1443.6 mm in 2015), shallow groundwater NH_4^+-N concentrations > 0.23 mg/l and a NO_3^- isotopic signature pointing towards low incomplete denitrification (for more information see Clagnan et al. (2018)). The shallow drainage system consists of tightly spaced gravel moles 1.5 m apart installed at 0.45 m connected to a 10 m spaced pipe drain system at 0.9 m (Fig. 1) (Clagnan et al., 2018). The soil profile consisted of the following depth and horizon classification and textures: 0 − 40 cm: Ap/O (clay loam with humic inferring this horizon had a higher % of organic matter (OM) than mineral matter), 41 − 62 cm: Btg (silty clay), 63 − 140 cm: Cg1 (silty clay loam) and 140–170 cm: Cg2 (silty clay loam)) (Tuohy et al., 2016).

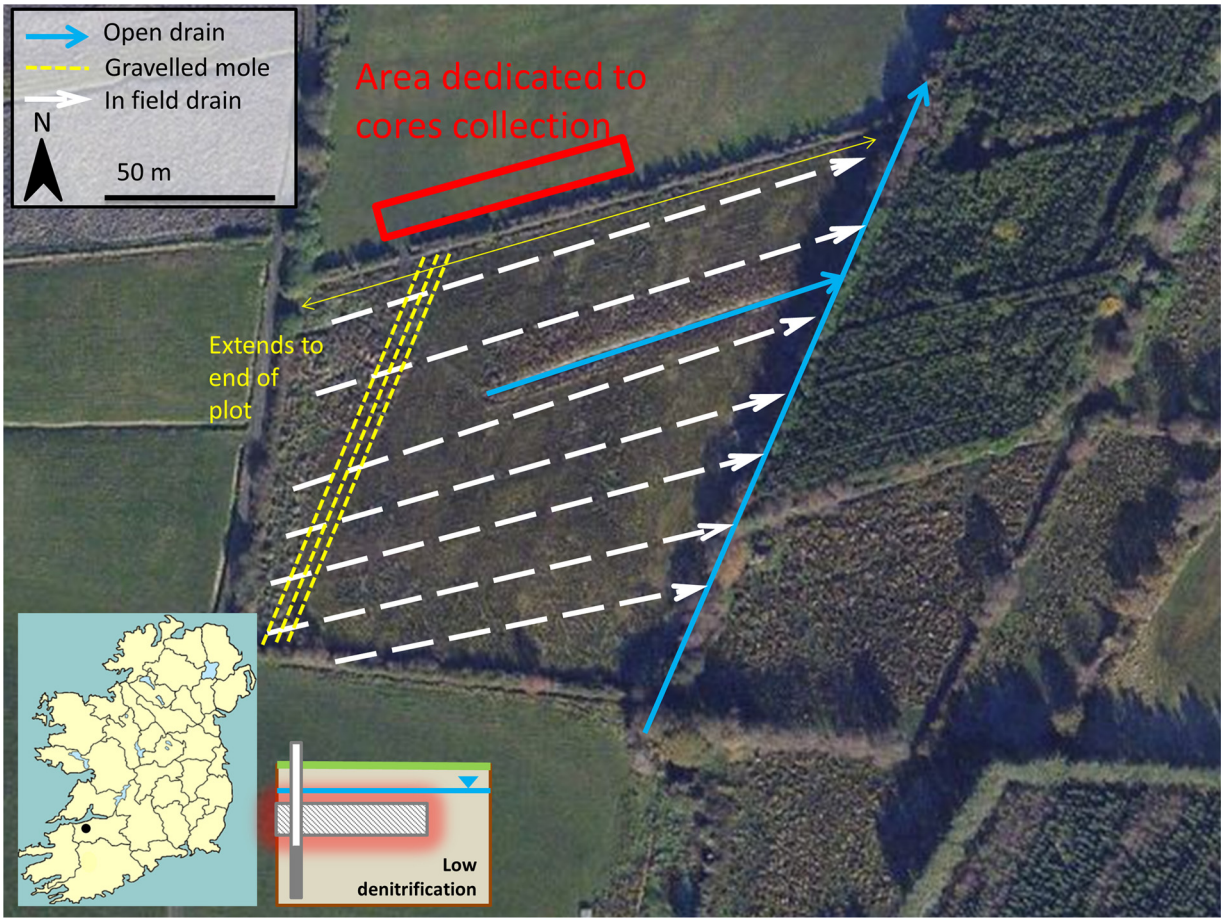

Fig. 1. Location of the site, drainage design and area demarcated where intact cores were excavated.

2.2. Core excavation

In February 2017, a total of 20 intact soil cores were collected to a depth of 0.45 m (Fig. 1) in an un-drained control section of the field. Each core consisted of a PVC tube (0.45 m length and 0.15 m of internal diameter) (Fig. 2). Cores were positioned carefully on the grass sod to cause minimal disturbance of the topsoil and grass cover during excavation (Fig. S1). Cores were then capped and transported to the Teagasc Johnstown Castle glasshouse facility. Here, grass was trimmed, the bottom 0.1 m of the soil profile was removed from the cores so that the top soil layer (Ap/O, clay loam) and a portion of the second soil layer (Btg, silty clay) were preserved. Three cm of gravel were then added to the bottom part of the cores and end caps were affixed and sealed to the bottom of each core using silicone. To monitor the water level within the core, a hole was drilled and later sealed to house a detachable transparent side tube. Petroleum jelly was heated and then poured down the sides of the soil core to seal any possible gap between the perimeter of the core and the PVC tube for the top 5 cm, and to avoid preferential flow along the sides. Three 2 cm diameter holes were created on the side of the intact cores and these were used to create the varied watertable height necessary for the saturated treatments. Cores were subjected to an adaptation period until each core achieved and

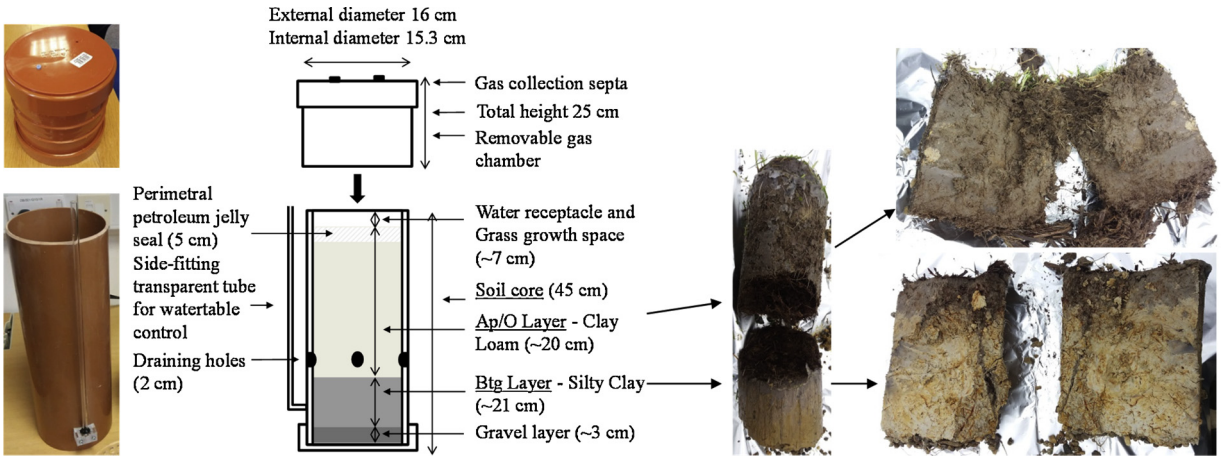

Fig. 2. Intact core apparatus, setup and soil core description.

maintained two targeted saturations (80% and 55% WFPS) for a period of 1 month. The WFPS was measured every other day through a ProCheck 5TE in-situ probe and distilled water was added to the top of the cores where necessary to maintain a constant WFPS. This simulated rainfall causing waterlogging conditions in surface water gley soils. For high WFPS, the holes were sealed for the duration of the experiment; for the low WFPS, the holes were left open for the duration of the experiment. Stainless steel mesh was used to cover the open holes to ensure no soil loss. During the adaptation period temperature inside the glass house was reflected outside temperatures.

2.3. Experimental conditions

Field site bulk density (BD) was calculated as 1.11 g/cm^3 in the top soil horizon. The selected targeted saturations were 80% and 55% WFPS. Actual conditions achieved were 79% for HS cores (standard deviation = 5.0%) and 51% for LS cores (standard deviation 2.7%). Based on Rafique et al. (2011), WFPS ranges from 30.4% to 85.2% over the summer months while it ranges from 49.1% to 99.5% over the winter months, with highest values recorded within heavy textured gley soils. The WFPS of LS was therefore selected from the values registered by Rafique et al. (2011) on heavy textured gley soils while for HS cores it corresponded to the highest WFPS value reached by our soil after 1 month of waterlogging.

The two saturations were calculated using the following equation: WFPS = ((GSMC*BD)/(1-(BD/PD))*100, where GMSC is the gravimetric soil moisture content (VSMC/BD) and PD is particle density (2.65 g/cm^3). The depth of water inside the cores was monitored daily using the outside tubing and volumetric soil moisture content (VSMC). Surface soil temperature and electrical conductivity (EC) were measured every 2 days for a month before and after fertiliser application using a ProCheck 5TE in-situ probe. During the running of the experiment, ambient temperature ranged between 9.6 and 23.0 °C with a similar variation encountered within the 0 − 5 cm of the soil cores (max: 23.9 °C, min: 8.1 °C).

Different core sets were subjected to three different fertiliser amendments. Two fertilisers consisted of differently labelled ammonium nitrate ($^{15}NH_4{}^{15}NO_3$ and $^{14}NH_4{}^{15}NO_3$) (50% atom enrichment) and a third control consisted of non-labelled ammonium nitrate ($^{14}NH_4{}^{14}NO_3$) fertilisation (Bateman and Baggs, 2005). The rate of fertiliser was 250 N kg/ha. Fertiliser was dissolved in distilled water and 30 ml of this solution were sprayed on the surface of the soil of each core with a 50 ml plastic syringe (different set of syringes were used for each treatment). Three cores for each treatment were used for each amendment and fertiliser was applied between day 0 and day 1 of sampling.

2.4. Gas analyses

In March 2017, gas samples were collected before (day 0) and at 1, 2, 3, 5, 7, 10, 14, 24 days after fertilisation. Gas chambers (15 cm diameter, 20 cm height) were created for gas sampling following guidelines for N_2O static chambers by Klein and Harvey (2012). Air tight gas chambers were fitted onto the top of the cores and samples were collected through rubber septa using 20 ml plastic syringes and needles. For N_2O, 20 ml gas samples were taken from the gas chambers of all the cores using gas tight syringes, at 0, 15, 30 min after chamber deposition. Samples were stored in 12 ml exetainers (LabcoWycomb Ltd., UK) which were previously evacuated and flushed with He. The N_2O was quantified by gas chromatography (CP-3800, Varian Inc. USA). Additional 20 ml samples were collected 2 h after chamber deposition, with the same methodology as for previous samples. These additional samples were collected from both the labelled and non-labelled cores for the analysis of ^{15}N-N_2O and ^{15}N-N_2. Samples were stored in 12 ml exetainers previously evacuated and flushed with He. In order to avoid gas leakage or contamination during storage, exetainers were individually stored upside down in water filled disposable plastic tubes. Isotopic compositions ($^{15}/^{14}N$) for N_2O and N_2 and N_2 quantification were determined at the UC Davis Stable Isotope Facility, Davis, California in June 2017 as per Mosier and Schimel, 1993 (Limit of Quantitation: N_2O - approx. 150 pmol, N_2 - approx. 150 nmol). Samples were shipped together with control samples. Additional 20 ml atmospheric samples were collected at the same time as the 2 hs samples and represents background values. N_2O fluxes were calculated following the equation:

$$\text{Flux} = (\text{dGas/dt}) \times 10 - 6 \times (V_{\text{chamber}} \times p \times 100 \times MW)/(R \times T) \times 103 \times (1/A)$$

where, dGas is the gas concentration change over time (dt) (ppm/h), V_{chamber} is the volume of the gas chamber used (0.003 m^3 in this study), p is the atmospheric pressure (hPa, measured with an EGM-4 Environmental Gas Monitor (PP Systems)), MW molecular weight (g/mol), R gas constant (8.314 J/mol/K), T is the temperature (K, measured in this study by the EGM-4 Environmental Gas Monitor (PP Systems)) and A is the area of the chamber.

Enrichments of N_2O and N_2 were calculated following different methods (i.e. Mosier and Schimel, 1993; Stevens and Laughlin, 1998, 2001; Bateman and Baggs, 2005). In more detail, N_2 enrichment was calculated as follows: $^{15}X_N = 2\ (\delta^{30}R/\delta^{29}R)/(1 + \delta^{30}R/\delta^{29}R)$ where $\delta^{29}R$ = ($^{29}N_2/^{28}N_2$ in enriched atmosphere - $^{29}N_2/^{28}N_2$ in normal air) and where $\delta^{30}R$ = ($^{30}N_2/^{28}N_2$ in enriched atmosphere - $^{30}N_2/^{28}N_2$ in normal air). The fraction (d) of the N_2 molecules derived from the labelled $NO_3{}^+$ pool (denitrification) was calculated from: $d = \delta^{30}R/(^{15}X_N)^2$. The amount of N_2 evolved was calculated as follows: N_2 evolved = d (N_2 in headspace/$(1 - d)$). The flux of N_2 evolved from the mix of added ^{15}N fertiliser and soil N at natural abundance was calculated as: Flux of $N_2 = N_{2\text{evolved}}/(A{\cdot}t)$ where A is the soil surface area covered by the chamber and t is time of deposition. Similarly, the N_2O enrichment was calculated as follows: Flux of $N_2O = N_2O_{\text{evolved}}/(A{\cdot}t)$. The ^{15}N-N_2O emissions evolved from the $^{14}NH_4{}^{15}NO_3$ were considered the result of denitrification, the emissions evolved from $^{15}NH_4{}^{15}NO_3$ of denitrification and nitrification (autotrophic and heterotrophic), while the ^{15}N-$N_2O{}^{15}NH_4{}^{15}NO_3$ emissions minus ^{15}N-$N_2O{}^{14}NH_4{}^{15}NO_3$ the result of nitrification.

2.5. Soil analyses

Soil samples were collected by destructively sampling the cores at multiple time periods: 1) early samples collected on site – February 2017, 2) two cores at the end of the one-month adaptation period – March 2017 and 3) all 18 cores receiving fertiliser at the end of the experimental period – April 2017. Two samples were collected from each core: one in the upper organic rich clay loam (Ap/O, soil organic matter (SOM): 59.6%) horizon and one in the lower heavier silty clay (Btg, SOM: 4.54%) horizon. All samples were dried for one week at 60 °C, sieved (≤ 2 mm) and then ball milled to produce a fine powder. The chemical analyses for pH, SOM and C and N % contents were conducted as follows: a 1:2.5 suspension of soil in water was created by mixing deionised water (25 ml) with the milled soil samples (10 ml) in a 50 ml polyethene tube, which was then shaken for 2 h on an orbital shaker (set to 160 rotations/min) after which pH was measured. Ceramic crucibles were filled with 4 g of soils, dried overnight at 105 °C and weighed (Reeuwijk, 2002). This process was repeated and then the samples were placed in a furnace (Nabertherm, Germany), burned at 500 °C, and weighed again. SOM was then calculated following the formula: SOM (% w/w) = (((Soil 105 °C (g) + Crucible (g)) – (Soil 500 °C + Crucible (g))/(Soil 105 °C (g)-Crucible (g)))*100.

For C% and N%, samples (approximately 0.2 g) were transferred into tin foil cups and then analysed through a LECO TruSpec CN elemental analyser. Soil samples at known C% and N% were used as standards. Soil C% and N% were then used to optimise sample weight

for soil enrichment (^{15}N) analyses. Samples where then encapsulated in tin capsules and ^{15}N contents were determined at the UC Davis Stable Isotope Facility, Davis, California, through a PDZ Europa ANCA-GSL elemental analyser interfaced with a PDZ Europa 20-20 isotope ratio mass spectrometer (Sercon Ltd., Cheshire, UK). Enrichment in soil was calculated following the method of Mosier and Shimel (1993). The amount of ^{15}N in soil was calculated through the following formula: amount of ^{15}N in soil = atom%^{15}N of soil total N/ 100 * total N in soil; while the amount of N derived from fertiliser as per: ^{15}N from fertiliser = total ^{15}N – control cores ^{15}N.

2.6. Grass analyses

Grass samples were collected at multiple time periods; 1) from the two cores that were destructed at the end of the adaptation period and 2) from all cores destructively sampled at the end of the experiment. A composite sample was created for each treatment. Grass was dried at 60 °C for 5 days within perforated plastic bags and then ground (≤ 0.2 mm) through a grass grinder. Samples were analysed for C% and N%. Samples (approximately 0.1 g) were transferred into tin foil cups and then analysed through a LECO TruSpec CN elemental analyser as per soil. Grass C% and N% were then used to optimise sample weight for grass enrichment (^{15}N) analyses as per soil. Enrichment in grass was calculated following Mosier and Shimel (1993). The total amount of ^{15}N in grass was calculated formulas follows: total ^{15}N in grass = total grass N * atom%^{15}N of grass / 100; while the amount of ^{15}N derived from fertiliser as per: ^{15}N from fertiliser = total ^{15}N – control cores ^{15}N.

Both grass and soil enrichment for the two treatments were used to calculate the ^{15}N fertiliser recovery rates as per: % of fertiliser N recovered = total ^{15}N derived from fertiliser/amount of ^{15}N applied *100; being the total ^{15}N derived from fertiliser the sum of ^{15}N from soil and ^{15}N from grass.

2.7. Soil gene abundances

Additional soil samples were collected with a sterile trowel for the two horizons from the holes left by the core extraction in the field. Three subsamples were taken randomly spaced across the exposed horizon layer and combined in a sterile sealable bag to create a composite soil sample. After homogenisation, these were immediately frozen in dry ice while in the field and stored at −80 °C at the end of each sampling day. Further soil samples were collected after condition and at the end of the experiment. Three replicates for each soil sample were extracted using a PowerSoil® DNA Isolation Kit (MoBio Laboratories, Inc, USA) according to manufacturer's guidance. Samples were visualized on 1% (w/v) 1 × TAE agarose gels and DNA was stored at −80 °C until analysis within 2 months from extraction. To quantify DNA from soil (number of copies per gram of dry soil), the dry-weight of the soil and the proportion of water to soil was accounted for through soil moisture analyses. To create a multiplication factor specific for each sample to convert the absolute estimation of copies into an estimation of copies per gram of dry soil, samples of soil were weighted before extraction and replicates of these samples were weighted before and after a period of 2 weeks at 80 °C.

Extracts were diluted 1:10 in Ambion® nuclease-free water (Thermo Fisher Scientific, Inc, USA) to reduce possible inhibition. Amplifications were realised using the SYBR Green PCR kit master mix (QIAGEN, Netherlands) according to manufacturer's instruction in a total volume of 15 µl. An aliquot of 3 µl of the 1:10 solution of template was added per reaction to the PCR master mix. Condition of the PCR followed the protocols outlined in the references of Table 1. The q-RT-PCR quantification was performed in triplicate for standards and in duplicate for extracts using an AB700 real-time PCR cycler according to manufacturer's instructions. Duplicates that showed a difference between threshold cycles (ΔCt) below 1 were considered acceptable. Samples that showed low amplification were purified using Microcon® PCR

Table 1
Genes and primer sets used for the qPCR of the soil samples collected from the cores.

Gene	Primer	Sequence (5'-3')	Amplicon size (bp)	Reaction condition	References
16S	F: 341 F	CCTACGGGAGGCAGCAG	194	95 °C-15 min; 40 cycles of 95 °C-20 sec, 54 °C-20 sec, acquisition at 72 °C-30 sec; 95 °C-10 sec; 60 °C-15 sec; dissociation curve. (Improved from Daniell et al., 2012)	Muyzer et al. (1993)
	R: 518R	ATTACCGCGGCTGCTGG			
nirK	F: nirK876	ATYGGCGGVCAYGGCGA	164	95 °C-15 min; 6 cycles of 95 °C-15 sec, 63 to 58 °C-30 sec with a decrease of 1 °C every cycle, 72 °C-30 sec, 80 °C-15 sec; 40 cycles of 95 °C-15 sec, 60 °C-30 sec, 72 °C-30 sec, acquisition at 80 °C-30 sec; 95 °C-15 sec; dissociation curve. (Henry et al., 2004)	Hallin et al. (2009)
	R: nirK1040	GCCTCGATCAGRTTRTGGTT			
nirS	F: Cd3aF	GTSAACGTSAAGGARACSGG	416	95 °C-10 min; 40 cycles of 95 °C-30 sec, 57 °C-20 sec, acquisition at 72 °C-30 sec; 95 °C-15 sec; dissociation curve. (Thompson et al., 2016)	Michotey et al. (2000) Throback et al. (2004)
	R: R3cd	GASTTCGGRTGSGTCTTGA			
nosZ1	F: nosZ2F	CGCRACGGCAASAAGGTSMSSGT	267	95 °C-15 min; 6 cycles of 95 °C-15 sec, 65 to 60 °C-30 sec with a decrease of 1 °C every cycle, 72 °C-30 sec, 80 °C-15 sec; 40 cycles of 95 °C-15 sec, 60 °C-15 sec, 72 °C-30 sec, acquisition at 80 °C-30 sec; 95 °C-15 sec; dissociation curve. (Henry et al., 2006)	Henry et al. (2006)
	R: nosZ2R	CARRTGCAKSGCRTGGCAGAA			
nosZ2	F: nosZ-II-F	CTIGGICCIYTKCAYAC	683	95 °C-15 min; 40 cycles of 95 °C-15 sec, 54 °C-30 sec, 72 °C-30 sec acquisition at 80 °C-30 sec; 95 °C-15 sec; dissociation curve. (Jones et al., 2013)	Jones et al. (2013)
	R: nosZ-II-R	GCIGARCARAAITCBGTRC			
amoA	F: amoA-1 F	GGGGTTTCTACTGGTGGT	491	95 °C-10 min; 45 cycles of 95 °C-1 min, 54 °C-1 min, acquisition at 72 °C-1 min; 72 °C-10 min; dissociation curve. (Segal et al., 2017)	Rotthauwe et al. (1997)
	R: amoA-2R	CCCCTCKGSAAAGCCTTCTTC			
hzo1	F: hzoF1	TGTGCATGGTCAATTGAAAG	740	95 °C-10 min; 40 cycles of 95 °C-30 sec, 56 °C-20 sec, acquisition at 72 °C-40 sec; 95 °C-15 sec; dissociation curve. (Kong et al., 2013)	Kong et al. (2013)
	R: hzoR1	CAACCTCTTCWGCAGGTGCATG			
nrfA	F: nrfAF2aw	CARTGYCAYGTBGARTA	269	95 °C-10 min; 50 cycles of 95 °C-15 sec, 52 °C-45 sec, 72 °C-20 sec acquisition at 80 °C-35 sec; 95 °C-15 sec; dissociation curve. (Song et al., 2014)	Welsh et al. (2014)
	R: nrfAR1	TWNGGCATRTGRCARTC			

grade filters (Merck Millipore, USA), no inhibition was however encountered.

Standard curves were produced for absolute quantifications of 16S rRNA, four bacterial denitrification genes (*nirS, nirK, nosZ1 and nosZ2*), one for bacterial nitrification (*amoA*), one for bacterial anammox (*hzo* cluster 1) and one for bacterial DNRA (*nrfA*). Plasmid (pGEMt for *16S rRNA, nirS, nirK, nosZ1, nosZ2* and *amoA* while PCR4-Topo for *hzo*) with an insert of the target genes, and genomic E. Coli MG1655 DNA for *nrfA*, were used as standards. Standard plasmid was quantified though the use of Qubit dsDNA BR Assay Kit following manufacturer's instructions. Triplicate curves were created using corresponding standards (from 10^9 to 10^1 copy numbers, 10-fold serial dilution series) and primer sets (Table 1). For all bacterial genes, results are presented as GCC per litre (GCC/l).

2.8. Statistical analyses

Significant differences of gas fluxes (N_2O and N_2), enrichment data and between abundance of N cycling genes and the 16S RNA gene was tested between treatments through the use of one way ANOVA and Tukey's HSD test (IBM SPSS Statistics version 24) ($\alpha = 0.05$). When an equal variance was not assumed, Dunnett's T3 test was used instead of Tukey's. Data was logarithmically transformed to ensure normality before analyses.

3. Results

3.1. N_2O emissions

Prior to the addition of fertiliser there was no significant difference between the two treatments. Background values of N_2O emission were in the range of 0.01 - 0.02 and 0.00 - 0.10 mg N_2O-N/m^2h for the HS and LS cores, respectively. Following fertilisation (day 0–1), values were significantly different ($p < 0.05$) between the two treatments until day 24. A steep increase was seen in the emission rate for the HS treatment which peaked after 5 days (11.97 mg N_2O-N/m^2h). The LS treatment showed a slower increase in the N_2O emission rate at a lower magnitude, which peaked between day 7 (1.64 mg N_2O-N/m^2h) and 14 (1.63 mg N_2O-N/m^2h) (Fig. 3).

3.2. N_2O and N_2 gas enrichment

The use of fertiliser with different isotopic labels was necessary in order to assess the contribution of denitrification and nitrification (Fig. 4). Compared with N_2O flux data, enrichment data showed a significant ($p < 0.05$) predominance of nitrification in the LS treatment between day 1 and 14. Denitrification accounted for 2.8–25.2% of the total N_2O emission while nitrification accounting for 74.8–97.2%. The ratio between these two processes remained almost constant across the duration of the experiment, with a slight decrease in denitrification after day 5 following fertilisation. The HS treatment showed a significantly higher contribution of the denitrification process to N_2O emission when compared with the LS treatment between day 1 and 10. On the day following fertilisation, denitrification accounted for 72.5–73.4% of emissions. Denitrification rate decreased from the start of the experiment, reaching minimum values of 18.8% at day 24 after fertilisation. Denitrification was the main producer of N_2O for the HS treatment until day 10 while nitrification for the LS treatment over the whole experimental period.

The N_2 flux increased from HS cores and by day 1 a N_2 flux of 6.3 mg N/m^2h increased to 30.3 mg N/m^2h by day 10 (Fig. S2). Usable data were obtained only from the HS cores ($^{15}NH_4{}^{15}NO_3$); LS treatments did not produce detectable N_2 amounts except for one recordable data of 0.8 (± 0.1) mg N/m^2h on day 1 (this data was still used for the calculation of contribution pathways). Additionally, no data were also recorded for HS after day 10 possibly due to a dilution of the enriched pool.

3.3. Soil and grass enrichment and recovery rates

The amount of ^{15}N in soil derived from the fertiliser was calculated for both soil (within the top 0 − 5 cm) and grass for both HS and LS treatments (Fig. S3). Within the $^{14}NH_4{}^{15}NO_3$ treatment, HS cores averaged 0.007 g ^{15}N while LS 0.026 g ^{15}N ($p < 0.05$). The same pattern, but without a significant difference, was evident for the $^{15}NH_4{}^{15}NO_3$ treatment, HS had values of 0.051 g ^{15}N while LS of 0.064 g ^{15}N. The same trend of higher enrichment within LS cores was exhibited for the grass composite samples, with values of 0.03 g ^{15}N and 0.36 g ^{15}N for the HS and LS cores of the $^{14}NH_4{}^{15}NO_3$ treatment, respectively. Results for the HS and LS core of the $^{15}NH_4{}^{15}NO_3$ treatment were 0.16 g ^{15}N and 0.55 g ^{15}N, respectively. These data were further used to calculate the ^{15}N fertiliser recovery rates for both soil and grass

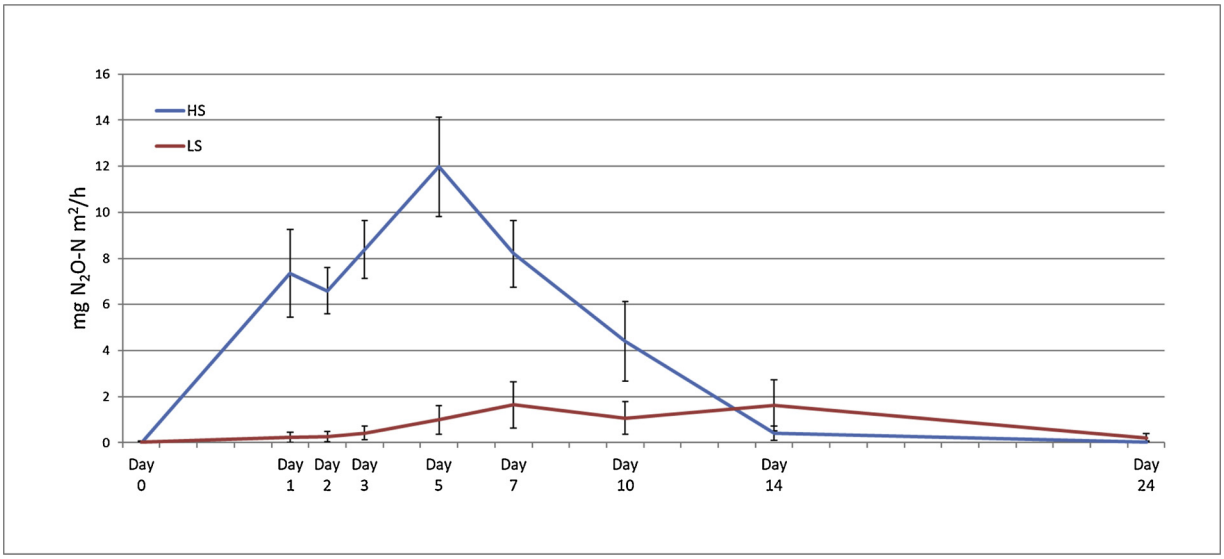

Fig. 3. Temporal patterns of N_2O-N emission rates from the HS (80% WFPS) and LS (50% WFPS) treatments following fertilisation (between day 0 and 1) with 250 N kg/ha of NH_4NO_3. Error bars represent standard deviation for high and low saturation treatments (n = 9).

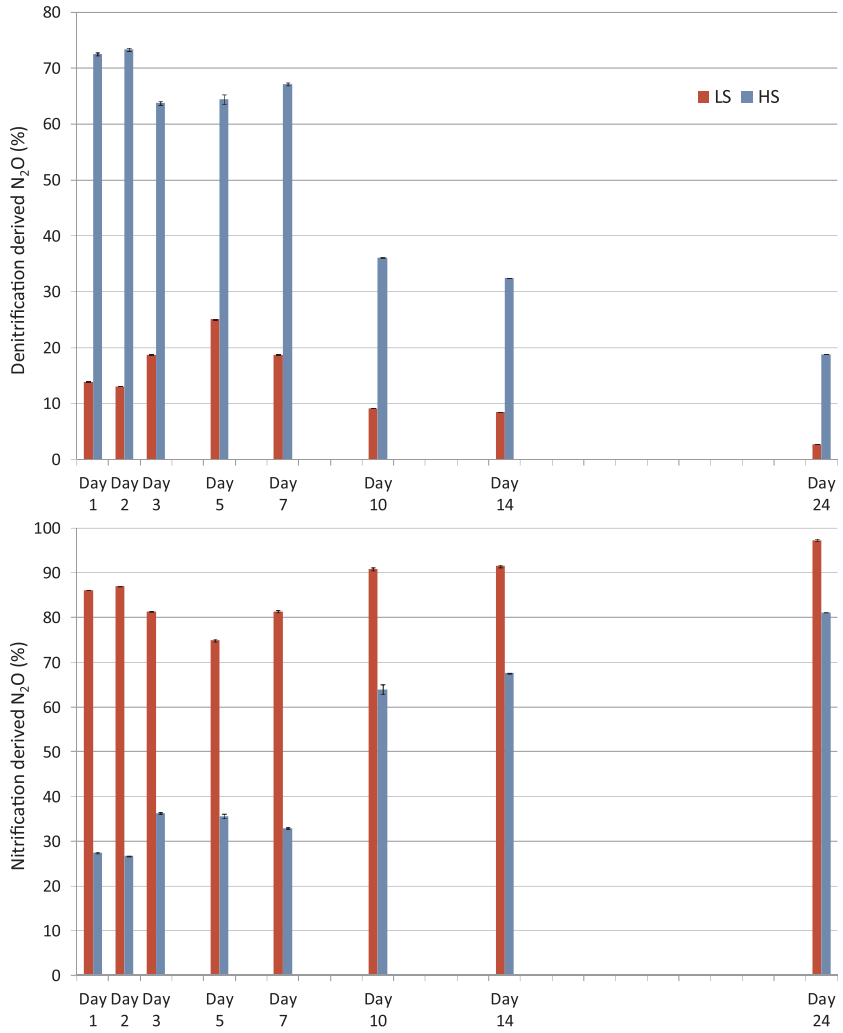

Fig. 4. Percentage of N_2O emissions from denitrification (top) and nitrification (bottom) for low (red) and high saturation (blue) treatments for the days following fertilisation. Standard deviations are indicated for high and low saturation treatment (n = 3).

for the treatment. $^{14}NH_4{}^{15}NO_3$ recovery rates were of 0.7% and of 6.1% for HS and LS, respectively. Results for $^{14}NH_4{}^{15}NO_3$ were 1.7% and of 4.9% for HS and LS treatments, respectively.

Considering all components, the two treatments showed differential patterns of apportionment (Fig. 5). The HS cores and LS cores showed similar N_2O emissions from nitrification (4.6% and 3.5% respectively, $p > 0.05$) when considering enrichment of N_2O emissions over the whole period. However, HS had a high component of N_2O derived from denitrification (6.0% HS vs. 0.4% LS, $p < 0.05$). A significant amount of N_2O was transformed to N_2 within HS cores, which showed 62.9% of the N was lost through N_2 production compared with 3.7% for the LS cores. Therefore, some N remains unaccounted for HS cores 23.9% and LS 84.7%.

3.4. Variation of GCC of genes across treatments

Gene abundances were analysed in a) samples collected at the time of core extraction in the field (F_{insitu}) and b) samples collected before the addition of the fertiliser from 80% (HS-i) and 50% saturation cores (LS-i) and again at the end of the experiment again from 80% (HS-f) and 50% saturation cores (LS-f).

Soils from the top layer showed higher GCC for the *16S* gene within LS-i treatment while significantly lower concentrations were found in HS-f and LS-f (Fig. 6, Table S1). The gene *nirS* showed lowest GCCs

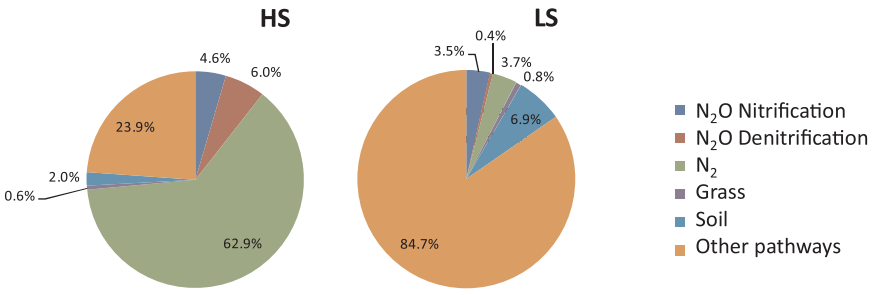

Fig. 5. Contribution of each N loss pathway for the HS and LS treatments.

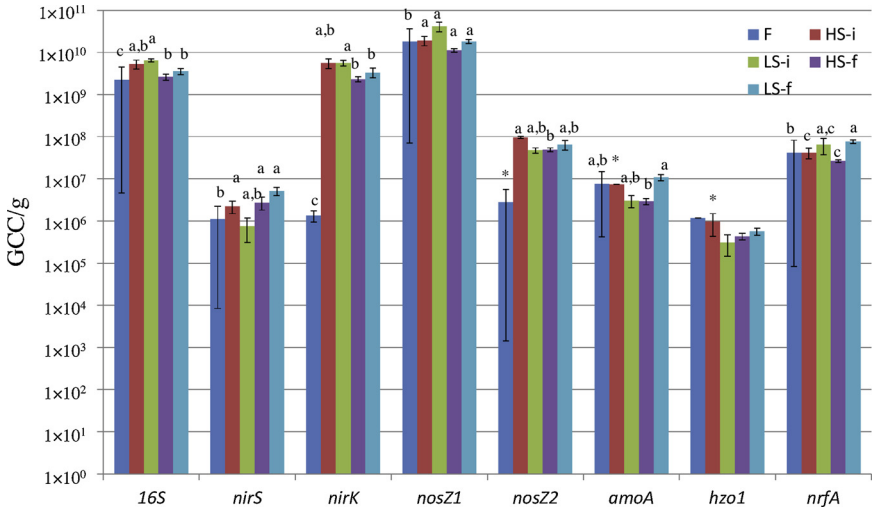

Fig. 6. Variation in gene copy concentration (GCC/l) in the topsoil for: samples collected within the field (F; n = 3) at the moment of core extraction, samples collected before the addition of fertiliser from the high (HS-i; n = 3) and low saturation treatment (LS-i; n = 3) and at the end of the experiment again from high (HS-f; n = 9) and low saturation cores (LS-f; n = 9). Standard errors are indicated for each separated gene group. Statistical differences ($p < 0.05$) between GCC are indicated by different letters within each gene group. Groups excluded from the analyses are indicated with *.

within F_{insitu}. The gene *nirK* showed higher GCCs than *nirS*; lowest GCC were found in F_{insitu} while LS-i presented highest GCC. Treatments LS-f and HS-f were significant different from LS-i. The gene for *nosZ1* was favoured over *nosZ2*. The gene *nosZ1* did not showed significantly different GCCs values across treatments except for F_{insitu}. The gene *nosZ2* showed significantly higher GCC in HS-i while lower in HS-f. The gene for *amoA* had higher GCC at LS-f while lowest at HS-f; other groups did not exhibit any statistical differences. The gene for *hzo1* showed no significant differences across groups. The gene for *nrfA* showed higher GCC in group LS-f and lower within group HS-f.

Soils from the bottom layer showed a lower GCC for the *16S* gene when compared to those from the top layer ($p < 0.05$). The GCC of *16S* varied between groups, higher GCCs were found within F_{insitu}, whilst lowest equivalent were found in HS-f and LS-f (Fig. 7, Table S2). Due to the low abundance found for the *16S* gene, analysis of the bottom layer was restricted to the most abundant genes found within the top layer (*nirK*, *nosZ1*, *amoA* and *nrfA*). The gene *nirK* followed the same pattern as for *16S*. The gene *nosZ1* had a similar pattern to *16S* with highest GCC at F_{insitu} and lowest only at HS-f. For the gene *amoA*, F_{insitu}, HS-f and LS-f were found to have statistically different GCC. The gene *nrfA* showed higher GCC in F_{insitu}, lower in HS-f.

4. Discussion

4.1. WFPS and fertiliser application versus N_2O and N_2 fluxes

Nitrification and denitrification are main processes within the N cycle and they are the cause of approximately 70% of global N_2O emissions from both agricultural and natural soils (Syakila and Kroeze, 2011; Braker and Conrad, 2011).

In terms of N_2O emissions, Rafique et al. (2011) found high variation in N_2O emissions over a two-year period among eight Irish intensive grasslands, as thresholds (levels of WFPS for the conversions of N_2O emissions to N_2) tend to vary among soil types. During summer, WFPS ranged from 30.3 to 85.2% while between 49.1 and 99.5% in winter, higher N_2O emissions were found on free draining brown and grey brown podzols (0.11 mg N_2O-N/m^2h) than poorly drained gley soils (0.07 mg N_2O-N/m^2h). Additionally, in a study on soil texture, silt loam soils had the highest N_2O emissions with emissions 80–158% higher than loamy sand soils and 100–282% higher than sandy loam soils (Gaillard et al., 2016). In two soil incubation studies with enriched fertiliser over 25 and 12 days respectively, Bateman and Baggs (2005) and Cardenas et al. (2017) found highest N_2O fluxes at 70% WFPS in a silty loam while at 80% WFPS in a silty clay loam. A WFPS below 20% was shown to be limiting for N_2O emissions; at a WFPS between 35% and 60% (range common to the LS cores), the N_2O production

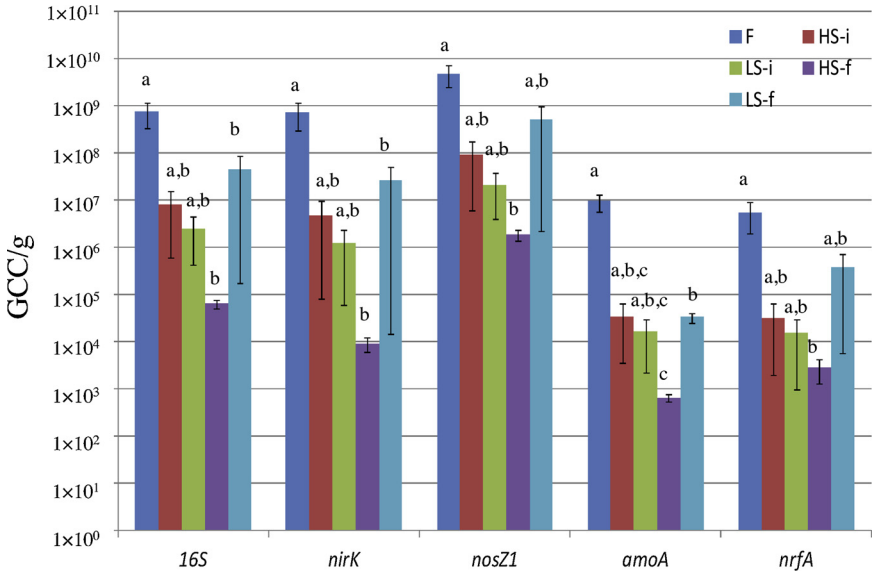

Fig. 7. Variation in gene copy concentration (GCC/l) at the base of the soil profile: samples collected within the field (F; n = 3) at the moment of core extraction, samples collected before the addition of fertilizer from high (HS-i; n = 3) and low saturation treatment (LS-i; n = 3) and at the end of the experiment again from high (HS-f; n = 9) and low saturation cores (LS-f; n = 9). Standard errors are indicated for each separated gene group. Statistical differences ($p < 0.05$) between GCC are indicated by different letters within each gene group.

constantly increased accordingly with the increase in WFPS reaching a peak between a WFPS of 60% and 80% (range common to the HS cores) (Rafique et al., 2011). Therefore, for the same texture, an increase of saturation (up to 80%) leads to increased N_2O emissions with a complete conversion to N_2 at the upper limit of WFPS. Fine textured soils produce greater total N_2O emissions than looser textured soils (clay soils emission are 1.5 times higher than that of sandy soils) (van Groenigen et al., 2004; Lesschen et al., 2011). Bateman and Baggs (2005) further found that almost only N_2 was produced above WFPS of 90%. In this study, WFPS of 90% could not be achieved and the cores were characterised by high N_2O emission under extreme WFPS conditions (HS, non-drained cores). Background N_2O-N emission fluxes found within this study were in the range of the background values registered by Rafique et al. (2011) for grassland on Irish poorly drained gley soils (clay loam) (i.e. average values: min. -0.055, max. 0.105 mg N_2O-N/m^2h) and by Abdalla et al. (2009) from a sandy loam grassland (average values: min. -0.03, max0.06 mg N_2O-N/m^2h), well above Irish well-drained soils (coarse loam over fine loam av.: 0.003 mg N_2O-N/m^2h) (Bourdin et al., 2014); loamy sand (unfertilised grassland) av.: 0.003 mg N_2O-N/m^2h) (Roth et al., 2013).

High N_2O fluxes were generally recorded (from clay loam soil cores) immediately after fertiliser application (Scholefeld et al., 1997). Within this study, N_2O emission values showed a spike, especially within the HS treatment following fertiliser application. Here the spike was reported from day 1–5 after fertilisation for the HS treatment and from day 3–14 for the LS treatment. This agrees with Hyde et al. (2006), which recorded an increase in N_2O emission within 1–2 weeks after fertilisation. Harty et al. (2016) recorded across three Irish sites that 78–80% of N_2O emissions above 0.125 mg N_2O-N/m^2h) occurred at 60–80% WFPS with higher N_2O emission values from imperfectly drained soil (clay loam: 0.092 mg N_2O-N/m^2h)) than well (sandy loam: 0.030 mg N_2O-N/m^2h)) or moderately well (sandy loam: 0.023 mg N_2O-N/m^2h)) drained soils after fertilisation with CAN. Di-nitrogen is not considered a GHG or a contamination and its measurement is challenging due to the high atmospheric background concentration (Bergstermann et al., 2011; Cardenas et al., 2017). In a study on Irish moderately well-drained fine loam soil, a field study by Baily et al. (2011) reported N_2 fluxes (8780 mg N/m^2 h (297 st.err.; Jun 2009) and 940 mg N/m^2h (330 st.err.; Mar 2010)) higher than the present study after the addition of 100 kg N/ha of fertiliser ($^{14}NH_4{}^{15}NO_3$). A 17-day incubation study by Jahangir et al. (2012) observed similar fluxes to the current study, that total denitrification and the N_2O mole fraction ($N_2O/(N_2O + N_2)$) both increased with soil depth, reflecting higher WFPS in subsoils. This is inline a field study by McGeough et al. (2012) on a sandy clay loam soil which observed that N_2 was the dominant end product with the N_2O mole fraction ($N_2O/(N_2O + N_2)$) ranging from 0.24 to 0.34. Within the present study, the HS treatment was dominated by N_2 which accounted for 63% of N loss.

4.2. N transformation apportionment

As the WFPS was kept constant over the duration of the experiment, N transformation apportionment could be assessed after fertilisation (Fig. 4 and Fig. 5). The LS treatments showed a high prevalence of a nitrification signal throughout the experiment. Significantly higher rates of denitrification were found in HS treatments during the days (1–7) immediately following fertilisation as half of N in the fertiliser is ready for denitrification when applying ammonium nitrate. Denitrification was replaced by higher levels of nitrification on the last days (10–24) of the experiment coinciding with the drop in N_2O emissions of the initial spike after fertilisation. The N transformation apportionment changed therefore due to the management of the cores. Mathieu et al. (2006) highlighted that, while during unsaturated conditions 60% of N_2O is produced by nitrification, under saturated conditions N_2O production by nitrification decreases to 10–15%. The LS treatment in the present study showed denitrification and nitrification rates values similar to the ones presented by Bateman and Baggs (2005) for 50% WFPS. As expected, the HS treatment showed high denitrification rates. However, the achieved rates were not 100% but instead 73% perhaps due to the experimental setup i.e. intact rather than disturbed cores. Intact cores are heterogeneous, layered with varying soil texture and permeability and have a different porosity than sieved equivalents and are of course more representative of emissions from the natural environment.

Most laboratory scale studies investigating the role of soil moisture and fluxes have been designed using disturbed sieved soils (e.g. Stres et al., 2008), which means that the structure of the soil column has been removed and represents non-field conditions (Banerjee et al., 2016). Furthermore, some studies use small cores limiting the focus to a specific soil horizon (Stres et al., 2008), which does not reflect the multi layered heterogeneity and complexity of the unsaturated zone.

The ^{15}N apportionment and recovery rates further highlighted the different ratios of the pathways of N transformation due to the denitrification spike within the HS vs. LS cores (Fig. 5). The ^{15}N that did not leave the column systems as gaseous emission of N_2O or N_2 was recovered within soil and grass, with a higher percentage of ^{15}N retained in soil within LS core, or possibly lost (i.e. other unaccounted pathways). The low accounted N_2, especially within the LS cores, is the result of a lower production of N_2. This low production was most likely enhanced by N_2 below level of detection (due to the high minimum detectable N_2 limits needed) and therefore unaccounted suggesting a possible over estimation of N losses. On the other hand, low N_2 emissions within the LS cores could be attributable to ^{15}N to moving deeper in the soil rather than lost through N_2, due to the lower soil moisture and therefore faster draining possibly leaching along subsurface pathways out of the 5 cm thickness that was analysed.

Additionally, ^{15}N could be further lost through NH_3 volatilisation as a minor loss pathway (NH_3 volatilisation and leaching pathways were not measured within this study). No significant difference was found in NH_3 emission on six Irish soil types (Burchill et al., 2016). Daily NH_3 emissions ranged from 0 to 5.58 kg N/ha peaking on the third day after fertilisation (Urea)(10–40% VWC) (Burchill et al., 2016). NH_3 emission increased with increasing temperature and decreasing soil moisture content (35–85% field capacity) occurring under both warm-dry conditions and cool-wet conditions (McGarry et al., 1987). Water content was found to be the main driver of NH_3 volatilization with higher emissions recorded at 50% WFPS rather than at 80% (Castellano-Hinojosa et al., 2019). At the same time 80% WFPS favoured denitrification, due to the limited O_2 availability. Additionally, the addition of fertiliser at this WFPS instead of at 50% has been shown to increase denitrification genes due to the higher availability of NO_3^- (Castellano-Hinojosa et al., 2019).

4.3. Variation of GCC of genes across treatments

The analysis of microbial communities has been coupled with the measurement of N_2O emissions only recently (Butterbach-Bahl et al., 2013). This often came with contrasting results as bacterial population has resulted in both clear (Philippot et al., 2009) or absent (Henry et al., 2008) correlations with N_2O emission. The combination of these techniques highlights the need for more insights in the partitioning of microbial N_2O sources in relation to a wide range of environmental condition (e.g. rewetting) to guide agriculture towards the production of lower and more sustainable amounts of gas emission (Butterbach-Bahl et al., 2013).

The influence of water content and flow velocities on microbial GCC was shown to be a driver for the definition of community structure and bacterial transport (Ruehle et al., 2015). The saturation level in natural systems varies continuously and is dependent on temporal changes (i.e. seasonal and meteorological patterns) and management, which create difficulties when demonstrating the link between communities, activity and environmental factors (Giles et al., 2012). Therefore, controlled

laboratory experiments offer more stable conditions to examine processes without such variability. The constant change of water conditions and saturation seem to select microbial populations with high resilience characteristics. These will maintain their structure over the long term but quickly respond to daily variation (i.e. respiration pulses) and seasonal dynamics (Waldrop and Firestone, 2006; Cruz-Martinez et al., 2009; Peralta et al., 2013). An increasing frequency of extreme weather events and changes in baseline conditions to levels outside the normal range can initiate longer-term changes in microbial population composition with the creation of distinct communities (Cruz-Martinez et al., 2009; Peralta et al., 2013).

All these data on bacterial communities are essential when trying to predict the possible effects of drainage installation or, the opposite, re-wetting on the occurring N transformation processes and losses. Herein, differences in GCCs were highlighted across most analysed genes (*16S*, *nirS, nirK*, *nosZ1*, *nosZ2*, *amoA* and *nrfA*) with the exception of *hzo1*. In all cases *nirK* was favoured over *nirS,* with *nosZ1* preferred over *nosZ2*. Both HS and LS treatments showed similar *nirK* GCCs and therefore similar potentials for N_2O production. The similar values for *nosZ1* gene highlighted within the HS and LS cores suggested a similar ability to transform N_2O to N_2, however *nosZ2* seemed to indicate a reduction of this ability from HS-i to HS-f cores. A reduction of GCCs for the HS-f cores when compared to LS-f cores was seen for the genes *amoA* and *nrfA*. Therefore, this highlighted a reduced potential for both nitrification and DNRA within HS-f cores.

4.4. Implications for re-wetting

In some countries re-wetting or the installation of control structures to manage water table heights have been shown to be effective at controlling N_2O emissions to decrease the N_2O:N_2 ratio in favour of more complete denitrification and N_2 production (Elmi et al., 2005).

Using an array of techniques and matching soil microbial potential with N_2O and N_2 emission and ^{15}N analyses for the contribution of nitrification and denitrification, this study explained the effect of drainage and rewetting in terms of gaseous emissions providing an explanation in terms of community switches.

The drainage of heavy textured soils is two-fold: it can reduce complete denitrification, thereby reducing N_2 transformation. However, it can also avoid high N_2O emissions. On the current soil type, control structures would push the system towards complete denitrification with only N_2 production (WFPS ~100%) but may present risks in terms of NH_3 emissions to the atmosphere and NH_4^+ losses to water. This should be investigated further in terms of willingness for farmers to adopt such a mitigation measure and cost effectiveness. In un-drained soil profiles, conditions in heavy textured soils are anaerobic resulting in the suppression of nitrification and complete attenuation of NH_4^+ (Aulakh et al., 1991). Artificially draining soils with lower hydraulic conductivities enables greater infiltration of water and DO into the soil profile, which may induce contamination and/or pollution swapping in shallow groundwater. Several studies (e.g. Necpalova et al., 2012; Clagnan et al., 2018) showed that, on heavy textured soils, elevated NH_4^+ and not NO_3^- was found at end-of-pipe, ditch and shallow groundwater locations.

5. Conclusions

Different patterns of N_2O and N_2 emissions and transformation processes were evident in 80% saturation intact cores. Pulses of N_2O and N_2 occurred and both nitrification and denitrification signals were identified. There was a definite increase in denitrification after fertilisation. This could lead to high ammonium leached losses, which could be a consequence of re-wetting on this soil type. In the 50% saturation treatment, the transformation process was dominated by nitrification with low N_2O and N_2 emissions. In the leached N pathway, there could be a reduction in NH_4^+ but a higher concentration of NO_3^-. Information collected from low saturation treatments showed that low WFPS produced low N_2O and N_2 emissions with a shift towards higher losses of N in groundwater (indicated by the large amount of non-apportioned N). High saturation cores showed a reduced potential for nitrification, complete denitrification and DNRA (lower GCCs than LS cores). However, the vast majority of N emissions were in the form of N_2 with a high component of N_2O due to pulses of denitrification when compared with low saturation cores. High saturation cores further showed a lower amount of unaccounted N, which highlights lower losses.

The authors whose names are listed immediately below certify that they have NO affiliations with or involvement in any organization or entity with any financial interest (such as honoraria; educational grants; participation in speakers' bureaus; membership, employment, consultancies, stock ownership, or other equity interest; and expert testimony or patent-licensing arrangements), or non-financial interest (such as personal or professional relationships, affiliations, knowledge or beliefs) in the subject matter or materials discussed in this manuscript.

Declaration of Competing Interest

The authors whose names are listed immediately below certify that they have NO affiliations with or involvement in any organization or entity with any financial interest (such as honoraria; educational grants; participation in speakers' bureaus; membership, employment, consultancies, stock ownership, or other equity interest; and expert testimony or patent-licensing arrangements), or non-financial interest (such as personal or professional relationships, affiliations, knowledge or beliefs) in the subject matter or materials discussed in this manuscript.

Acknowledgements

The study was funded by the Teagasc Walsh Fellowship Scheme under the RMIS No. 6707JC in collaboration with the Department of Civil and Structural Engineering, University of Sheffield. Special thank goes to the landowner Mr. J. Leahy for facilitating access to the farm and helping with core collection. Thanks also to the Heavy Soil Programme team in Moorepark. Thanks to Mr. P. Blackbourn at the University of Sheffield for the creation of the cores and extraction device. Thanks to Mrs. C. O'Connor for laboratory assistance and soil analyses in Johnstown Castle.

Appendix A. Supplementary data

Supplementary material related to this article can be found, in the online version, at doi:https://doi.org/10.1016/j.still.2019.104543.

References

Abdalla, M., Jones, M., Smith, P., Williams, M., 2009. Nitrous oxide fluxes and denitrification sensitivity to temperature in Irish pasture soils. Soil Use Manage. 24, 376–388.

Allison, S.D., Martiny, J.B.H., 2008. Resistance, resilience, and redundancy in microbial communities. Proc. Natl. Acad. Sci. USA 105, 11512–11519.

Aulakh, M.S., Doran, J.W., Mosier, A.R., 1991. Field-evaluation of four methods for measuring denitrification. Soil Sci. Soc. Am. J. 55, 1332–1338.

Baily, A., Rock, L., Watson, C.J., Fenton, O., 2011. Spatial and temporal variations in groundwater nitrate at an intensive dairy farm in south-east Ireland: insights from stable isotope data. Agric. Ecosyst. Environ. 144, 308–318.

Baily, A., Watson, C.J., Laughlin, R., Matthews, D., McGeough, K., Jordan, P., 2012. Use of the ^{15}N gas flux method to measure the source and level of N_2O and N_2 emissions from grazed grassland. Nutr. Cycling Agroecosyst. 94 (2-3), 287–298.

Bateman, E.J., Baggs, E.M., 2005. Contributions of nitrification and denitrification to N_2O emissions from soils at different water-filled pore space. Biol. Fertil. Soils 41, 379–388.

Banerjee, S., Helgasonb, B., Wang, L.F., Winsley, T., Ferrari, B.C., Siciliano, S.D., 2016. Legacy effects of soil moisture on microbial community structure and N2O emissions. Soil Biol. Biochem. 95, 40–50.

Bergstermann, A., Cárdenas, L., Bol, R., Gilliam, L., Goulding, K., Meijide, A., Scholefield, D., Vallejo, A., Well, R., 2011. Effect of antecedent soil moisture conditions on emissions and isotopologue distribution of N2O during denitrification. Soil Biol. Biochem. 43 (2), 240–250.
Bourdin, F., Sakrabani, R., Kibblewhite, M.G., Lanigan, G.J., 2014. Effect of slurry dry matter content, application technique and timing on emissions of ammonia and greenhouse gas from cattle slurry applied to grassland soils in Ireland. Agric. Ecosyst. Environ. 188, 122–133.
Braker, G., Conrad, R., 2011. Diversity, structure, and size of N_2O-producing microbial communities in soils - what matters for their functioning? Adv. Appl. Microbiol. 75, 33–70.
Bu, C., Wang, Y., Ge, C., Ahmad, H.A., Gao, B., Ni, S.-Q., 2017. Dissimilatory nitrate reduction to ammonium in the Yellow River Estuary: rates, abundance, and community diversity. Sci. Rep. 7, 6830.
Burchill, W., Lanigan, G.J., Forrestal, P.J., Reville, F., Misselbrook, T., Richards, K.G., 2016. A field-based comparison of ammonia emissions from six Irish soil types following urea fertiliser application. Irish J. Agric. Food Res. 55 (2), 152–158.
Butterbach-Bahl, K., Baggs, E.M., Dannenmann, M., Kiese, R., Zechmeister-Boltenstern, S., 2013. Nitrous oxide emissions from soils: how well do we understand the processes and their controls? Philos. Trans. Biol. Sci. 368, 20130122.
Cardenas, L.M., Bol, R., Lewicka-szczebak, D., Stuart, A., 2017. Effect of soil saturation on denitrification in a grassland soil. Biogeosciences 14, 4691–4710.
Castellano-Hinojosa, A., González-López, J., Vallejo, A., Bedmar, E.J., 2019. Linking ammonia volatilization with moisture content and abundance of nitrification and denitrification genes in N-fertilized soils. In: Zúñiga-Dávila, D., González-Andrés, F., Ormeño-Orrillo, E. (Eds.), Microbial Probiotics for Agricultural Systems. Sustainability in Plant and Crop Protection. Springer, Cham.
Clagnan, E., Thornton, S.F., Rolfe, S.A., Tuohy, P., Peyton, D., Wells, N.S., Fenton, O., 2018. Influence of artificial drainage system design on the nitrogen attenuation potential of gley soils: evidence from hydrochemical and isotope studies under field-scale conditions. Environ. Manage. 206, 1028–1038.
Cruz-Martinez, K., Suttle, K.B., Brodie, E.L., Power, M.E., Andersen, G.L., Banfield, J.F., 2009. Despite strong seasonal responses, soil microbial consortia are more resilient to long-term changes in rainfall than overlying grassland. ISME J. 3, 738–744.
Daniell, T.J., Davidson, J., Alexander, C.J., Caul, S., Roberts, D.M., 2012. Improved real-time PCR estimation of gene copy number in soil extracts using an artificial reference. J. Microbiol. Methods 91 (1), 38–44.
Decock, C., Six, J., 2013. How reliable is the intramolecular distribution of ^{15}N in N_2O to source partition N2O emitted from soil? Soil Biol. Biochem. 65, 114–127.
Elmi, A., Burton, D., Gordon, R., Madramootoo, C., 2005. Impacts of water table management on N_2O and N_2 from a sandy loam soil in Southwestern Quebec, Canada. Nutr. Cycling Agroecosyst. 72 (3), 229–240.
Enwall, K., Throback, I.N., Stenberg, M., Soderstrom, M., Hallin, S., 2010. Soil resources influence spatial patterns of denitrifying communities at scales compatible with land management. Appl. Environ. Microbiol. 76, 2243–2250.
Fierer, N., Schimel, J.P., Holden, P.A., 2003. Variations in microbial community composition through two soil depth profiles. Soil Biol. Biochem. 35, 167–176.
Gaillard, R., Duval, B.D., Osterholz, W.R., Kucharik, C.J., 2016. Simulated effects of soil texture on nitrous oxide emission factors from corn and soybean agroecosystems in Wisconsin. J. Environ. Qual. 45, 1540–1548.
Giles, M., Morley, N., Baggs, E.M., Daniell, T.J., 2012. Soil nitrate reducing processes - Drivers, mechanisms for spatial variation, and significance for nitrous oxide production. Front. Microbiol. 3, 1–16.
Groffman, P.M., Altabet, M.A., Böhlke, J.K., Butterbach-Bahl, K., David, M.B., Firestone, M.K., Giblin, A.E., Kana, T.M., Nielsen, L.P., Voytek, 2006. Methids for measuring denitrification: diverse approaches to a difficult problem. Ecol. Appl. 16 (6), 2091–2122.
Hallin, S., Jones, C.M., Schloter, M., Philippot, L., 2009. Relationship between N-cycling communities and ecosystem functioning in a 50-year-old fertilization experiment. ISME J. 3 (5), 597–605.
Harty, M.A., Forrestal, P.J., Watson, C.J., McGeough, K.L., Carolan, R., Elliot, C., Krol, D., Laughlin, R.J., Rchards, K.G., Lanigan, G.J., 2016. Reducing nitrous oxide emissions by changing N fertiliser use from calcium ammonium nitrate (CAN) to urea based formulations. Sci. Total Environ. 563–564, 576–586.
Henry, S., Baudoin, E., Lopez-Gutierrez, J.C., Martin-Laurent, F., Brauman, A., Philippot, L., 2004. Quantification of denitrifying bacteria in soils by nirK gene targeted real-time PCR. J. Microbiol. Methods, 59, 327-335. Corrigendum (2005) 61, 289–290.
Henry, S., Bru, D., Stres, B., Hallet, S., Philippot, L., 2006. Quantitative detection of the nosZ gene, encoding nitrous oxide reductase, and comparison of the abundances of 16S rRNA, narG, nirK, and nosZ genes in soils. Appl. Environ. Microbiol. 72 (8), 5181–5189.
Henry, S., Texier, S., Hallet, S., Bru, D., Dambreville, C., Cheneby, D., Bizouard, F., Germon, J.C., Philippot, L., 2008. Disentangling the rhizosphere effect on nitrate reducers and denitrifiers: insight into the role of root exudates. Environ. Microbiol. 10, 3082–3092.
Humbert, S., Tarnawski, S., Fromin, N., Mallet, M.P., Aragno, M., Zopfi, J., 2010. Molecular detection of anammox bacteria in terrestrial ecosystems: distribution and diversity. ISME J. 4 (3), 450–454.
Hyde, B.P., Hawkins, M.J., Fanning, A.F., Noonan, D., Ryan, M., O'Toole, P., Carton, O.T., 2006. Nitrous oxide emissions from a fertilized and grazed grassland in the south east of Ireland. Nutr. Cycling. Agroecosyst. 75, 187–200.
Jahangir, M.M.R., Khalil, M.I., Johnston, P., Cardenas, L., Hatch, D., Butler, M., Richards, K.G., 2012. Total denitrification potential in subsoils: a mechanism to reduce nitrate leaching to groundwater. Agric. Ecosyst. Environ. 147, 13–23.
Jones, C.M., Graf, D.R., Bru, D., Philippot, L., Hallin, S., 2013. The unaccounted yet abundant nitrous oxidereducing microbial community: a potential nitrous oxide sink. ISME J. 7 (2), 417–426.
Klein, C., Harvey, M., 2012. Nitrous Oxide Chamber Methodology Guidelines. Ministry for Primary Industries, New Zealand, pp. 1–145.
Knowles, R., 1982. Denitrification. Microbiol. Rev. 46 (1), 43–70.
Kong, L., Jing, H., Kataoka, T., Buchwald, C., Liu, H., 2013. Diversity and spatial distribution of hydrazine oxidoreductase (hzo) gene in the oxygen minimum zone off Costa Rica. PLOS ONE. 8 (10), e78275.
Lesschen, J.P., Velthof, G.L., de Vries, W., Kros, J., 2011. Differentiation of nitrous oxide emission factors for agricultural soils. Environ. Pollut. 159 (11), 3215–3222.
Long, A., Heitman, J., Tobias, C., Philips, R., Song, B., 2013. Co-occurring anammox, denitrification, and codenitrification in agricultural soils. Appl. Environ. Microbiol. 79 (1), 168–176.
Mathieu, O., Hénault, C., Lévêque, J., Baujard, E., Milloux, M.J., Andreux, F., 2006. Quantifying the contribution of nitrification and denitrification to the nitrous oxide flux using 15N tracers. Environ. Pollut. 144 (3), 933–940.
McGarry, S.J., O'Toole, P., Morgan, M.A., 1987. Effects of soil temperature and moisture content on ammonia volatilization from urea-treated pasture and tillage soils. Irish J. Agric. Res. 26, 173–182.
McGeough, K.L., Laughlin, R.J., Watson, C.J., Mueller, C., Ernfors, M., Cahalan, E., Richards, K.G., 2012. The effect of cattle slurry in combination with nitrate and the nitrification inhibitor dicyandiamide on in situ nitrous oxide and dinitrogen emissions. Biogeosciences 9, 4909–4919.
Michotey, V., Mejean, V., Bonin, P., 2000. Comparison of methods for quantification of cytochrome cd(1)denitrifying bacteria in environmental marine samples. Appl. Environ. Microbiol. 66, 15641571.
Morrissey, E.M., Jenkins, A.S., Brown, B.L., Franklin, R.B., 2013. Resource availability effects on nitrate reducing microbial communities in a freshwater wetland. Wetlands 33 (2), 301–310.
Mosier, A.R., Schimel, D.S., 1993. Nitrification and denitrification. In: Knowles, R., Blackburn, T.H. (Eds.), Nitrogen Isotope Techniques. Academic Press, Orlando, FL, pp. 181–208.
Muyzer, G., Waal, E.C.D.E., Uitierlinden, A.G., 1993. Profiling of complex microbial populations by denaturing gradient gel electrophoresis analysis of polymerase chain reaction-amplified genes coding for 16S rRNA. Appl. Environ. Microbiol. 59 (3), 695–700.
Necpalova, M., Fenton, O., Casey, I., Humphreys, J., 2012. N leaching to groundwater from dairy production involving grazing over the winter on a clay-loam soil. Sci. Total Environ. 432, 159–172.
Rafique, R., Hennessy, D., Kiely, G., 2011. Nitrous oxide emission from grazed grassland under different management systems. Ecosystems 14 (4), 563–582.
Peralta, A.L., Ludmer, S., Kent, A.D., 2013. Hydrologic history influences microbial community composition and nitrogen cycling under experimental drying/wetting treatments. Soil Biol. Biochem. 66, 29–37.
Philippot, L., Cuhel, J., Saby, N.B.A., Cheneby, D., Chronakova, A., Bru, D., Arrouays, D., Martin-Laurent, F., Simek, M., 2009. Mapping field-scale spatial patterns of size and activity of the denitrifier community. Environ. Microbiol. 11, 1518–1526.
Reeuwijk, L.P., 2002. Procedures for Soil Analysis, 6th ed. International Soil Reference and Information Centre.
Regan, K., Kammann, C., Hartung, K., Lenhart, K., Muller, C., Philippot, L., Kandeler, E., Marhan, S., 2011. Can differences in microbial abundances help explain enhanced N_2O emissions in a permanent grassland under elevated atmospheric CO_2? Global Change Biol. 17, 3176–3186.
Roth, B., Jones, M., Burke, J., Williams, M., 2013. The effects of land-use change from grassland to miscanthus x giganteus on soil N_2O emissions. Land 2 (3), 437–451.
Ruehle, F.A., Zentner, N., Stumpp, C., 2015. Changes in water table level influence solute transport in uniform porous media. Hydrol. Process. 29 (6), 875–888.
Scholefeld, D., Hawkins, J.M.B., Jackson, S.M., 1997. Use of a flowing helium atmosphere incubation technique to measure the effects of denitrification controls applied to intact cores of a clay soil. Soil Biol. Biochem. 29 (9-10), 1337–1344.
Segal, L.M., Miller, D.N., McGhee, R.P., Loecke, T.D., Cook, K.L., Shapiro, C.A., Drijber, R.A., 2017. Bacterial and archaeal ammonia oxidizers respond differently to long-term tillage and fertilizer management at a continuous maize site. Soil Till Res. 168, 110–117.
Song, K., Lee, S.H., Mitsch, W.J., Kang, H., 2010. Different responses of denitrification rates and denitrifying bacterial communities to hydrologic pulsing in created wetlands. Soil Biol. Biochem. 42, 1721–1727.
Song, B., Lisa, J.A., Tobias, C.R., 2014. Linking DNRA community structure and activity in a shallow lagoonal estuarine system. Front. Microbiol. 5, 1–10.
Stevens, R.J., Laughlin, R.J., 1998. Measurement of nitrous oxide and di-nitrogen emissions from agricultural soils. Nutr. Cycling Agroecosys. 52, 131–139.
Stevens, R.J., Laughlin, R.J., 2001. Lowering the detection limit for dinitrogen using the enrichment of nitrous oxide. Soil Biol. Biochem. 33, 1287–1289.
Stempfhuber, B., Welzl, G., Wubet, T., Schöning, I., Marhan, S., Buscot, F., Kandeler, E., Schloter, M., 2014. Drivers for ammonia-oxidation along a land-use gradient in grassland soils. Soil Biol. Biochem. 69, 179–186.
Stres, B., Danevčič, T., Pal, L., Fuka, M.M., Resman, L., Leskovec, S., Hacin, J., Stopar, D., Mahne, I., Mandic-Mulec, I., 2008. Influence of temperature and soil water content on bacterial, archaeal and denitrifying microbial communities in drained fen grassland soil microcosms. FEMS Microbiol. Ecol. 66 (1), 110–122.
Syakila, A., Kroeze, C., 2011. The global nitrogen budget revisited. Greenhouse Gas Meas. Manage. 1, 17–26.
Throback, I.N., Enwall, K., Jarvis, A., Hallin, S., 2004. Re-assessing PCR primers targeting nirS, nirK and nosZ genes for community surveys of denitrifying bacteria with DGGE. FEMS Microbiol. Ecol . 49, 401–417.
Tuohy, P., Humphreys, J., Holden, N.M., O'Loughlin, J., Reidy, B., Fenton, O., 2016. Visual drainage assessment: a standardised visual soil assessment method for use in

land drainage design in Ireland. Irish J. Agric. Food Res. 55 (1), 24–35.
Tuohy, P., O'Loughlin, J., Peyton, D., Fenton, O., 2018. The performance and behavior of land drainage systems and their impact on field scale hydrology in an increasingly volatile climate. Agric. Water Manage. 210, 96–107.
van Groenigen, J.W., Kasper, G.J., Velthof, G.L., Dasselaar, A.V.D.P., Kuikman, P.J., 2004. Nitrous oxide emissions from silage maize fields under different mineral nitrogen fertilizer and slurry applications. Plant Soil 263, 101–111.
Waldrop, M.P., Firestone, M.K., 2006. Seasonal dynamics of microbial community composition and function in oak canopy and open grassland soils. Microb. Ecol. 52 (3), 470–479.
Well, R., Augustin, J., Davis, J., Griffith, S.M., Meyer, K., Myrold, D.D., 2001. Production and transport of denitrification gases in shallow ground water. Nutr. Cycl. Agroecosyst. 60 (1–3), 65–75.
Welsh, A., Chee-Sanford, J.C., Connor, L.M., Löffler, F.E., Sanford, R.A., 2014. Refined NrfA phylogeny improves PCR-based nrfA gene detection. Appl. Environ. Microbiol. 80 (7), 2110–2119.
Yang, W.H., Silver, W.L., 2011. Application of the N_2/Ar technique to measure soil-atmosphere N_2 fluxes. Rapid Commun. Mass Spectrom. 26, 449–459.